Dissecting the roles of GRK2 and GRK3 in μ-opioid receptor internalization and β-arrestin2 recruitment using CRISPR/Cas9-edited HEK293 cells

Authors:

Thor C. Møller[1,3*], Mie F. Pedersen[1,3], Jeffrey R. van Senten[1], Sofie D. Seiersen[1], Jesper M. Mathiesen[1], Michel Bouvier[2], Hans Bräuner-Osborne[1*].

[1]*Department of Drug Design and Pharmacology, University of Copenhagen, 2100 Copenhagen, Denmark.*

[2]*Department of Biochemistry and Molecular Medicine, Institute for Research in Immunology and Cancer, Université de Montréal, Montreal, QC, Canada*

[3]These authors contributed equally to this work

*Co-corresponding authors: thor.moller@sund.ku.dk; hbo@sund.ku.dk

Abstract

Most G protein-coupled receptors (GPCRs) recruit β-arrestins and internalize upon agonist stimulation. For the μ-opioid receptor (μ-OR), this process has been linked to development of opioid tolerance. GPCR kinases (GRKs), particularly GRK2 and GRK3, have been shown to be important for μ-OR recruitment of β-arrestin and internalization. However, the contribution of GRK2 and GRK3 to β-arrestin recruitment and receptor internalization, remain to be determined in their complete absence. Using CRISPR/Cas9-mediated genome editing we established HEK293 cells with knockout of GRK2, GRK3 or both to dissect their individual contributions in β-arrestin2 recruitment and μ-OR internalization upon stimulation with four different agonists. We showed that GRK2/3 removal reduced agonist-induced μ-OR internalization and β-arrestin2 recruitment substantially and we found GRK2 to be more important for these processes than GRK3. Furthermore, we observed a sustained and GRK2/3 independent component of β-arrestin2 recruitment to the plasma membrane upon μ-OR activation. Rescue expression experiments restored GRK2/3 functions. Inhibition of GRK2/3 using the small molecule inhibitor CMPD101 showed a high similarity between the genetic and pharmacological approaches, cross-validating the specificity of both. However, off-target effects were observed at high CMPD101 concentrations. These GRK2/3 KO cell lines should prove useful for a wide range of studies on GPCR function.

Introduction:

The family of G protein-coupled receptors (GPCRs) constitute important drug targets, through which ~30% of all clinically approved medicines mediate their action[1]. Regulation of GPCR signaling following receptor activation is a complex process that typically involves recruitment of

37 kinases that phosphorylate the receptor to increase the receptor affinity for β-arrestins and
38 mediate receptor internalization[2]. The μ-opioid receptor (μ-OR) belongs to the family of
39 rhodopsin-like (family A) GPCRs and mediates the analgesic effects of opioid drugs, but also
40 related side-effects and addictive properties[3,4]. The regulation of μ-OR desensitization and
41 trafficking has been suggested to be linked to the development of tolerance after chronic use of
42 opioid drugs[5] and it is therefore important to understand the underlying molecular mechanisms.
43 Several studies indicate that receptor phosphorylation by GPCR kinases (GRKs) is important for
44 the desensitization of μ-OR signaling and initiation of internalization[6–12]. Out of the seven isotypes
45 in the GRK family, four (GRK2, GRK3, GRK5 and GRK6) have been speculated to regulate μ-OR *in*
46 *vivo* due to their overlapping expression patterns[13]. Knockout (KO) models have confirmed the
47 importance of the individual GRKs. For instance, it has been demonstrated that fentanyl and
48 morphine-induced tolerance are decreased in GRK3 KO mice[14], morphine reward and dependence
49 are lost in mice depleted of GRK5, but not GRK3, and morphine-induced locomotor activity is
50 increased in mice lacking GRK6 compared to wild type littermates[15,16]. Altogether, these studies
51 suggest that phosphorylation of μ-OR by specific GRK subtypes differentially impacts the
52 physiological outcome upon stimulation with opioids. The role of GRK2 has not been addressed in
53 KO systems due to lethal effects of removing GRK2 in mouse embryos[17]. Instead, the role of GRK2
54 has been studied using e.g. perfusion of a GRK2-inhibitory peptide or overexpression of a GRK2
55 dominant negative mutant in rat neurons, both demonstrating a role of GRK2 in μ-OR
56 desensitization[18,19].
57 Further insights into the mechanisms behind the role of GRKs in μ-OR pharmacology have
58 been obtained from *in vitro* studies. An early study demonstrated that phosphorylation of the μ-
59 OR could be increased by GRK2 overexpression, which led to increased β-arrestin recruitment and

60 μ-OR internalization[20]. The involvement of μ-OR phosphorylation in these processes was
61 confirmed by later studies[10,21–24]. In addition to GRK2, *in vitro* studies have shown that GRK3/5/6
62 have direct roles in μ-OR phosphorylation and/or internalization[16,23,25–27]. Moreover, studies have
63 also utilized phospho-site specific antibodies to demonstrate that the μ-OR is differentially
64 phosphorylated by distinct GRK isotypes depending on the agonist used. For instance, stimulation
65 with the full agonist D-Ala(2)-mephe(4)-gly-ol(5))enkephalin (DAMGO) leads to phosphorylation of
66 T370, S375, T376 and T379 in mouse μ-OR whereas stimulation with morphine – a full agonist for
67 G protein signaling, but a partial agonist for β-arrestin recruitment and μ-OR internalization[25] –
68 only leads to phosphorylation of S375[23,26]. In the same studies, the relative contribution of
69 GRK2/3/5/6 to μ-OR phosphorylation was also dependent on the agonist used.
70 The tools to study the involvement of GRKs in cell systems, have for now been restricted
71 mainly to short-interfering RNA techniques[10,23,26], the usage of dominant negative mutants of
72 GRK2[10,20,28] and utilization of Takeda compound 101 (CMPD101), a reported GRK2/3 selective
73 inhibitor[10,29–31]. To the best of our knowledge, no studies have investigated the role of GRKs in μ-
74 OR internalization in cell systems with complete KO of specific GRKs, which would prevent
75 incomplete knockdown of expression, residual kinase activity or unwanted overexpression effects.
76 Here, we report construction of individual and double KO of GRK2 and GRK3 cell lines in the
77 human embryonic kidney 293A (HEK293A) background, which we employ to investigate the
78 agonist-induced μ-OR internalization and β-arrestin2 recruitment in response to four different
79 agonists. We find that KO of GRK2 and GRK3 reduces agonist-induced μ-OR internalization and β-
80 arrestin2 recruitment. Additionally, we used a combination of β-arrestin2 recruitment assays that
81 either report β-arrestin2 proximity to μ-OR or to the cell membrane to identify a sustained and
82 GRK2/3 independent β-arrestin2 recruitment to the cell membrane. Furthermore, we present a

83 side-by-side comparison of the effects obtained with CMPD101 to the responses obtained in
84 GRK2/3 double KO cells. We find highly similar results with the two approaches when 10 μM of
85 CMPD101 is used; higher CMPD101 concentrations lead to non-GRK2/3-mediated effects. The cell
86 lines provide full KO of two important regulators of GPCR function and we expect them to be
87 useful tools for future studies of GPCR function.
88
89 **Results**
90 **Validation of GRK2 and/or GRK3 genome-edited HEK293A cells**
91 Construction of individual and combined GRK2 and GRK3 KO HEK293A cells (ΔGRK2, ΔGRK3 and
92 ΔGRK2/3) were performed using the clustered regularly interspaced short palindromic repeats
93 (CRISPR)/CRISPR associated protein 9 (Cas9) technology. Clones containing modification of all
94 alleles were identified with insertions or deletions in the *ADRBK1* locus (GRK2) and/or the *ADRBK2*
95 locus (GRK3) leading to frameshifts as shown by sequencing and indel detection by amplicon
96 analysis (IDAA)[32]. Furthermore, we confirmed the absence of full-length GRK2 protein expression
97 in the ΔGRK2 and ΔGRK2/3 cells and of full-length GRK3 protein expression in the ΔGRK3 and
98 ΔGRK2/3 cells using GRK2- and GRK3-selective antibodies (**Fig. 1**). No alteration of GRK2
99 expression in the ΔGRK3 clone or GRK3 expression in the ΔGRK2 clone compared to parental cells
100 could be detected (**Fig. 1**). Similarly, the expression of GRK5 and GRK6 was comparable in the
101 parental cells and the three ΔGRK cell lines (**Supplementary Fig. S2**).
102
103 **GRK2 and GRK3 contributes to μ-OR internalization**
104 We used a real-time internalization assay to determine the influence of GRK2 and GRK3 on μ-OR
105 internalization. This assay is based on time-resolved Förster resonance energy transfer (TR-FRET)

106 between a long lifetime donor (Lumi4-Tb) covalently linked to an amino-terminal SNAP-tag on cell
107 surface μ-OR and a cell impermeant acceptor (fluorescein) in the extracellular buffer[33,34].
108 Internalization separates the donor and acceptor molecules thus preventing energy transfer and
109 increasing the ratio of donor over acceptor emissions (internalization ratio). We compared the
110 ability of four μ-OR agonists to stimulate internalization: DAMGO, loperamide, fentanyl and
111 morphine. All four agonists induced internalization in a concentration-dependent manner and
112 reached a plateau between 45 and 90 min after agonist addition in the parental HEK293A cells as
113 well as in the ΔGRK2, ΔGRK3 and ΔGRK2/3 cell lines (**Fig. 2, Supplementary Fig. S3**).
114 Internalization was clearly reduced in the ΔGRK cells stimulated with DAMGO, loperamide and
115 fentanyl. A similar tendency was observed for morphine, but the effect was less clear compared to
116 the three other agonists due to lower overall internalization levels upon morphine stimulation. A
117 cell line where β-arrestin1 and -2 have been deleted in the same cellular background as the ΔGRK
118 cell lines has previously been described[35]. None of the agonists were able to induce internalization
119 in the Δβ-arrestin1/2 cell line (**Fig. 2, Supplementary Fig. S3**). We used the area under the curve
120 from the 90 min real-time internalization ratio traces to plot concentration-response curves and
121 determine the maximum response (E_{max}) and potency (EC_{50}) for the four agonists in each of the
122 cell lines where internalization could be detected (**Fig. 2, Table 1**). DAMGO stimulation led to a
123 higher E_{max} in the parental cells than stimulation with fentanyl and loperamide, which was larger
124 than the E_{max} upon morphine stimulation (**Fig. 2e**). For DAMGO, fentanyl and loperamide, we
125 found a decrease in E_{max} compared to the parental cells of 48-62% and 22-23% in the ΔGRK2 and
126 the ΔGRK3 cell lines, respectively. The E_{max} was further reduced, but not completely abolished in
127 the ΔGRK2/3 cell line and corresponded approximately to the sum of the reductions in the
128 individual ΔGRK2 and ΔGRK3 cell lines. The responses to morphine stimulation were too small for

129 in-depth quantitative analysis. Importantly, the μ-OR surface expression in the ΔGRK2 and/or -3
130 cell lines was similar or slightly higher than in the parental cells (**Fig. 2g**). More DNA was required
131 for transfection of the ΔGRK3 (30 ng/ml) and the ΔGRK2/3 (20 ng/ml) cell lines compared to the
132 parental and the ΔGRK2 (15 ng/ml) cell lines to achieve this. To determine whether the reduced
133 internalization was due to off-target effects of the single guide RNAs (sgRNAs) we overexpressed
134 the deleted GRKs in the corresponding cell lines. GRK2 or -3 overexpression restored the
135 internalization ratio to the levels of the parental cells, thus showing that the internalization
136 machinery is fully functional in the ΔGRK cell lines (**Supplementary Fig. S4**).
137
138 **GRK2 and GRK3 deletion reduces β-arrestin2 recruitment**
139 To further investigate the mechanism linking GRK2/3 and μ-OR internalization we measured the
140 recruitment of β-arrestin2 to μ-OR in the ΔGRK2 and/or -3 cells using a bioluminescence
141 resonance energy transfer 1 (BRET[1]) assay. In this assay, BRET between *Renilla reniformis*
142 luciferase II (RlucII)-tagged β-arrestin2 and μ-OR tagged with EYFP at the C-terminus is measured
143 in real-time. DAMGO, fentanyl and loperamide stimulation induced a peak in β-arrestin2
144 recruitment at 6 min for DAMGO and at 6-12 min for fentanyl and loperamide followed by a
145 gradual decrease in recruitment in the parental and ΔGRK3 cells (**Fig. 3**). The responses were
146 strongly decreased in the ΔGRK2 and ΔGRK2/3 cell lines and in most cases too small to discern the
147 kinetic profiles, except in the ΔGRK2 cells with DAMGO stimulation where a similar time-course
148 was observed. The response for morphine was too low to detect a peak in the β-arrestin2
149 recruitment. Since the kinetic profile was similar for all conditions where the response was
150 sufficiently large, we used the 6 min peak response to generate concentration-response curves for
151 determination of the maximum responses (E_{max}) and EC_{50} values for the β-arrestin2 recruitment

152 (**Supplementary Fig. S5, Supplementary Table S1**). In the parental HEK293A cells, DAMGO
153 stimulation led to the highest maximum response (E_{max}), followed by loperamide, fentanyl and
154 morphine stimulation. The E_{max} in the ΔGRK3 cells was similar to the parental cells, but reduced to
155 19-25% of the E_{max} in the parental cells in the ΔGRK2 cells stimulated with DAMGO and
156 loperamide. The β-arrestin2 recruitment in the ΔGRK2 cells stimulated with fentanyl and
157 morphine and in the ΔGRK2/3 cells stimulated with all ligands was too low for robust curve fitting
158 and in most cases no increase was seen even at the highest ligand concentrations. In the absence
159 of agonist stimulation, the β-arrestin2 recruitment was similar in all four cell lines (**Supplementary**
160 **Fig. S5**).
161 We further investigated the β-arrestin2 recruitment to μ-OR using an enhanced bystander
162 BRET (ebBRET) assay[36]. Here, BRET between β-arrestin2-RlucII and a membrane anchored *R.*
163 *reniformis* GFP (rGFP) increases as β-arrestin2 is recruited to the membrane. Importantly, the C-
164 terminus of the receptor is not modified for this assay and the amount of μ-OR DNA used for
165 transfection could be reduced by around 20-fold compared to the μ-OR-EYFP assay described
166 above while maintaining a good assay window. In agreement with the μ-OR-EYFP assay, β-
167 arrestin2 recruitment was similar in the parental and the ΔGRK3 cells and clearly decreased in the
168 ΔGRK2 and ΔGRK2/3 cell lines after 6 min stimulation with DAMGO, fentanyl and loperamide (**Fig.**
169 **4**). The maximum responses (E_{max}) in the ΔGRK2 and ΔGRK2/3 cells were 51-59% and 38-42%,
170 respectively, of the E_{max} in the parental cells (**Table 2**). These values are comparable to the
171 corresponding E_{max} values in the internalization assay, but higher than the μ-OR-EYFP β-arrestin2
172 recruitment assay. Increasing the amount of μ-OR DNA used for transfection in the ebBRET assay
173 to an amount comparable to the μ-OR-EYFP assay did not reduce the responses in the ΔGRK2 and
174 ΔGRK2/3 cell lines (**Supplementary Fig. S6**). Rescue expression of either GRK2 or GRK3 in the three

175 ΔGRK cell lines increased β-arrestin2 recruitment to the level of the parental cells with
176 overexpression of the same GRK for all four ligands (**Supplementary Fig. S7**).
177
178 **Sustained and GRK2/3 independent recruitment of β-arrestin2 to the plasma membrane**
179 We have previously observed that a considerable amount of β-arrestin2 recruitment can be
180 detected in the ebBRET assay after 60 min of μ-OR stimulation[25]. To determine if there is a kinetic
181 component to the effect of GRK2 and/or -3 knockout we measured the β-arrestin2 recruitment in
182 the ebBRET assay after 60 min stimulation in the genome-edited cell lines. There was a substantial
183 increase in β-arrestin2 recruitment at high agonist concentrations (**Supplementary Fig. S8**),
184 although the recruitment in the parental cells was slightly lower after 60 min than after 6 min
185 stimulation (**Fig. 5a,b**). The E_{max} values in the parental cells followed the same distribution as
186 observed after 6 min stimulation (**Supplementary Fig. S8**) and the EC_{50} values were similar to the
187 values obtained after 6 min stimulation (**Supplementary Table S2**). However, β-arrestin2
188 recruitment was unchanged in the ΔGRK2 and/or -3 cell lines relative to the parental cells, with
189 the exception of the ΔGRK3 cell line where DAMGO stimulation led to a 40% increased
190 recruitment. In contrast, the agonist-induced β-arrestin2 recruitment to μ-OR-EYFP was almost
191 reduced to buffer levels after 60 min stimulation (**Fig. 5c,d**). To get further insights into the
192 mechanism behind this difference we used a third β-arrestin2 recruitment assay where
193 recruitment of GFP^2-β-arrestin2 (BRET acceptor) to μ-OR-RlucII (BRET donor) is measured by
194 $BRET^2$. The results of this assay were overall in good agreement with the μ-OR-EYFP assay (**Fig.
195 5e,f**). Recruitment of GFP^2-β-arrestin1 to μ-OR-RlucII yielded results similar to recruitment of
196 GFP^2-β-arrestin2 (**Supplementary Fig. S9**).
197 Finally, we looked at the kinetic profile of the effect of GRK deletion on μ-OR internalization.

198 We initially analyzed the μ-OR internalization by taking the area under the curve of the 90 min
199 time curves, which could mask kinetic effects. However, concentration-response curves composed
200 from the μ-OR internalization responses after 6, 12, 30 and 60 min stimulation were highly similar
201 for all curves displaying sufficient signal-to-noise (**Supplementary Fig. S10**), thus indicating that
202 the effect of GRK2/3 knockout on μ-OR internalization is constant over time.
203
204 **Similar effects of genetic deletion and pharmacological inhibition of GRK2/3**
205 The small molecule inhibitor CMPD101 has been shown to selectively inhibit GRK2/3 over GRK1
206 and GRK5 *in vitro*[30]. We compared the internalization and β-arrestin2 recruitment results obtained
207 in the ΔGRK2/3 cells with that obtained using the kinase inhibitor. We used the ebBRET assay with
208 6 min stimulation to measure the β-arrestin2 recruitment. At CMPD101 concentrations ≤ 10 μM,
209 we observed no effect on receptor internalization in absence of agonist (basal internalization) (**Fig.**
210 **6a**) or basal β-arrestin2 recruitment (**Fig. 6e**) in the parental HEK293A and ΔGRK2/3 cells. With
211 DAMGO stimulation in the parental cells, we found a concentration dependent decrease in μ-OR
212 internalization (**Fig. 6b**) and β-arrestin2 recruitment (**Fig. 6f**) that plateaued at levels similar to the
213 ΔGRK2/3 cells with IC_{50} values of 1.8 μM (pIC_{50} = 5.79 ± 0.12) for internalization and 0.95 μM
214 (pIC_{50} = 6.03 ± 0.02) for β-arrestin2 recruitment at CMPD101 concentrations ≤ 10 μM. Thus, in this
215 concentration range CMPD101 specifically inhibits GRK2/3 and reaches inhibition comparable to
216 the ΔGRK2/3 cell line at 10 μM.
217 CMPD101 concentrations ≥ 30 μM decreased basal and DAMGO-stimulated μ-OR
218 internalization in both parental and ΔGRK2/3 cells (**Fig. 6a,b**). In contrast, basal and DAMGO
219 induced β-arrestin2 recruitment were constant over the range of CMPD101 concentrations tested
220 (up to 100 μM) in parental and ΔGRK2/3 cells (**Fig. 6e,f**). μ-OR surface expression was similar in

221 the parental and ΔGRK2/3 cells in the internalization and β-arrestin2 recruitment experiments
222 (**Fig. 6c,g**). Due to the long-lifetime donor fluorophore with several emission peaks and the
223 homogenous format, the internalization assay is sensitive to compounds that absorb light in most
224 of the visual spectrum. However, the donor signal in absence of acceptor was unaffected by
225 CMPD101 up to concentrations of 100 μM (**Fig. 6d**), demonstrating that the observed effects at
226 high concentrations were not due to optical interference with the internalization assay. We
227 conclude that CMPD101 at concentrations ≥ 30 μM has a non-GRK2/3 regulatory effect on basal
228 and agonist-stimulated μ-OR internalization.
229
230 **Discussion**
231 Compelling evidence on the importance of GRKs in μ-OR pharmacology has increased over the
232 years. Yet, most of these studies has relied on methods either overexpressing dominant negative
233 forms of the protein of interest or silencing with siRNAs, possibly leading to undesired effects of
234 overexpression or incomplete removal of the target protein[37]. Genome editing is a promising
235 alternative to these approaches to investigate the role of GRKs as potential modulators of GPCR
236 function. In this study we have generated genome-edited HEK293 cells and used them to dissect
237 the role of GRK2 and GRK3 in μ-OR internalization and β-arrestin2 recruitment.
238 Previous studies have demonstrated that GRK2 and GRK3 affect the phosphorylation state of
239 the ^{375}STANT^{379} motif in mouse μ-OR[22,23,26], and this region has been directly linked to the
240 regulation of μ-OR internalization by mutational studies[23,24]. Here, we demonstrate that our
241 ΔGRK2, ΔGRK3 and ΔGRK2/3 cell lines are excellent novel tools to dissect the role of these GRK
242 subtypes in DAMGO, fentanyl and loperamide-induced μ-OR internalization. Double KO of GRK2/3
243 had an additive effect on μ-OR internalization with a significant reduction for DAMGO-, fentanyl-

244 and loperamide-induced μ-OR internalization (**Fig. 2**, **Table 1**). No statistically significant difference
245 could be reached for morphine-induced μ-OR internalization, however this agonist induced low μ-
246 OR internalization and thereby the effects could be masked by the small assay window. Our study
247 also shows that there are additional factors controlling μ-OR internalization, since deletion of
248 GRK2/3 did not fully inhibit μ-OR internalization. There is limited evidence suggesting that GRK5 or
249 GRK6 could be responsible for this: μ-OR internalization is sensitive to GRK5 and GRK6
250 overexpression[16,25] and GRK5 has been shown to be important in HEK293 cells and mouse brain
251 for morphine-induced phosphorylation of Ser375[26], which is a critical residue in initiating further
252 C-terminal μ-OR phosphorylation[23]. In contrast, DAMGO-induced phosphorylation of the C-
253 terminal region of μ-OR was shown to be unaffected by knockdown of GRK5 and GRK6[23,26] and
254 fentanyl-induced Ser375 phosphorylation was unchanged in mice lacking GRK5[15], so the roles of
255 GRK5 and GRK6 might depend on the GRK expression levels in an individual cell. Several other
256 kinases and enzymes have been proposed to regulate μ-OR internalization, including
257 phospholipase D2 (PLD2) and protein kinase C (PKC)[5], but more studies are required to determine
258 their role relative to the GRKs. Our successful generation of the ΔGRK2, ΔGRK3 and ΔGRK2/3 cell
259 lines demonstrate the utility in this approach and calls for generation of additional cell lines
260 deficient of other kinases to dissect other contributors to μ-OR internalization in the future.
261 We observed a discrepancy between the two assays where β-arrestin2 recruitment is
262 measured using an EYFP or RlucII tag on the C-terminal end of the receptor and the ebBRET assay
263 where β-arrestin2 recruitment is measured using a BRET acceptor tethered to the membrane (**Fig.
264 5**). The two main differences between the assays is the presence or absence of a C-terminal tag on
265 μ-OR and the measurement of β-arrestin2 proximity to μ-OR or the cell membrane. Although C-
266 terminal tagging of μ-OR has previously been shown not to affect the μ-OR signaling in HEK293

267 cells or the behavior of knock-in mice[27] and we obtained similar results with two different tags, it
268 cannot be ruled out that the tags could interfere with the GRK and/or β-arrestin interaction with
269 μ-OR. Another potential explanation for the observed sustained β-arrestin recruitment to the cell
270 membrane is that there is a GRK2/3 independent component in addition to the GRK2/3 dependent
271 β-arrestin recruitment. This GRK2/3 independent component is only transiently associated with μ-
272 OR and remains associated with the cell membrane after dissociation from μ-OR. Such a
273 mechanism has previously been shown for several receptors, including μ-OR[38–40], and has been
274 suggested to result from an interaction where arrestin only engages the core of the receptor 7TM
275 bundle[38,40–42]. This interaction model would be consistent with our observation that the β-arrestin
276 population that remains associated with the cell membrane interacts with μ-OR independently of
277 GRK2/3. Our results would suggest that the combination of direct and bystander β-arrestin
278 recruitment assays that measure receptor and cell membrane proximity at different time points
279 could be used to discriminate transient and stable β-arrestin interactions.
280 Although using CRISPR/Cas9 genome editing to generate cell lines lacking specific proteins has
281 several advantages over conventional methods for interrogating protein function, it has also been
282 criticized for potentially selecting clones that have compensated for the lack of the deleted
283 protein[43]. We addressed this concern by reintroduction of the deleted proteins (**Supplementary**
284 **Figs. S4**, **S7**) and by pharmacological inhibition with CMPD101 (**Fig. 6**). Transient expression of
285 GRK2 or GRK3 showed that μ-OR in the genome-edited cells was still sensitive to regulation by
286 GRK2 and GRK3. Comparison with pharmacological inhibition is an alternative way to characterize
287 genome-edited cells if a specific and potent inhibitor exists. We compared the μ-OR internalization
288 and β-arrestin2 recruitment in the ΔGRK2/3 cells with the effect of the inhibitor CMPD101 on the
289 parental cells and found highly similar results. Collectively, these results demonstrate that there

290 are no significant compensatory mechanisms in the ΔGRK2/3 cells of relevance to the μ-OR
291 functions studied here and confirms the utility of CMPD101 as a GRK2/3 selective pharmacological
292 tool in concentrations up to 10 μM. Our ΔGRK2/3 cells also proved to be a powerful tool to study
293 specificity of GRK inhibitors as we could demonstrate off-target effects of CMPD101 at
294 concentrations ≥ 30 μM (**Fig. 6a,b**), which is a concentration range commonly used to inhibit
295 GRK2/3[10,31], thus cautioning the use of such high concentrations in future studies.
296 In conclusion, we have generated novel ΔGRK2, ΔGRK3 and ΔGRK2/3 cell lines in the highly
297 utilized HEK293A cell background. These cell lines complement the range of G protein and β-
298 arrestin cell lines generated by Dr. Asuka Inoue[44] and thus expand this highly efficient tool box to
299 study intracellular proteins involved in GPCR function and signaling. Here, we demonstrate the
300 utility of the cell lines to study μ-OR-mediated β-arrestin2 recruitment to the cell membrane and
301 μ-OR internalization, but we envision that the cell lines could be used for a range of other studies
302 and thus welcome all requests to obtain the ΔGRK2, ΔGRK3 and ΔGRK2/3 cell lines for future
303 studies.
304
305 **Methods**
306 **Materials**
307 Dulbeccos's modified Eagle medium (DMEM, Cat# 61965-026), fetal bovine serum (FBS), Opti-
308 MEM, Penicillin-Streptomycin, Dulbecco's phosphate buffered saline (DPBS, Cat# 14190-144),
309 Hank's balanced salt solution (HBSS, Cat# 14175-053), restriction endonucleases, TOPO TA cloning
310 kit for sequencing including TOP10 *E. coli.*, FastAP alkaline phosphatase, Pierce BCA Protein Assay
311 Kit, dithiothreitol, PageRuler Plus Prestained Protein Ladder (10 to 250 kDa), Pierce 10x Tris-
312 Glycine SDS Buffer, NuPAGE LDS Sample buffer (4x), SuperSignal West Pico PLUS and ELISA Femto

313 chemiluminescent substrates, and Pluronic F-68 non-ionic surfactant were purchased from
314 Thermo Fisher Scientific (Waltham, MA, USA). QuickExtract DNA Extraction Solution was
315 purchased from Lucigen Corporation (WI, USA) and TEMPase Hot Start DNA Polymerase from
316 Ampliqon (Odense, Denmark). Anti-GRK2 antibody (Cat# MAB43391, RRID:AB_2818985) and anti-
317 GRK5 antibody (Cat# AF4539, RRID:AB_2248068) were obtained from R&D Systems (Minneapolis,
318 MN, USA). Anti-GRK3 antibody (Cat# 80362, RRID:AB_2799951), anti-GRK6 antibody (Cat# 5878,
319 RRID:AB_11179210), and anti-rabbit IgG antibody conjugated to horseradish peroxidase (HRP)
320 (Cat# 7074, RRID:AB_2099233) were acquired from Cell Signaling Technology (Danvers, MA, USA).
321 Anti-GAPDH (Cat# NB600-502, RRID:AB_10077682) antibody was bought from Novus Biologicals
322 (Centennial, CO, USA). Anti-mouse IgG antibody conjugated to HRP (Cat# P0447,
323 RRID:AB_2617137) and anti-goat IgG antibody conjugated to HRP (Cat# P0449, RRID:AB_2617143)
324 were obtained from Agilent Technologies (Santa Clara, CA, USA). Mini-PROTEAN TDX Precast
325 Protein Gels and Trans-Blot Turbo RTA Mini PVDF Transfer Kit were purchased from Bio-Rad
326 Laboratories (Hercules, CA, USA). T4 PNK and T4 ligase were purchased from New England Biolabs
327 (Ipswich, MA, USA). Plasmid-Safe ATP-Dependent DNase was purchased from Epicentre
328 Technologies Corp. (Madison, WI, USA). Primers and sgRNA sequences were purchased from TAG
329 Copenhagen (Copenhagen, Denmark). FuGene6 Transfection Reagent was purchased from
330 Promega (Madison, WI, USA). Polyethylenimine (PEI) was purchased from Polysciences Inc.
331 (Warrington, PA, USA). Coelenterazine 400a and coelenterazine h were purchased from Cayman
332 Chemical Company (Ann Arbor, MI, USA). Tag-lite SNAP Lumi4-Tb was purchased from Cisbio
333 (Codolet, France). DAMGO was purchased from Abcam (Cambridge, United Kingdom). Anti-FLAG
334 M2 antibody (Cat# F3165, RRID:AB_259529), morphine sulfate, fentanyl citrate, and loperamide
335 hydrochloride, RIPA buffer, cOmplete protease inhibitor cocktail, Cell Dissociation Solution,

336 protease inhibitor cocktail, Trizma base, skim milk powder, and Tween 20 were purchased from
337 Sigma-Aldrich (St. Louis, MO, USA). CMPD101 was purchased from Tocris Bioscience (Bristol, UK).
338
339 **Plasmids**
340 The following plasmids were described previously: pcDNA5/FRT/TO-FLAG-SNAP-μ-OR[25],
341 pcDNA3.1(+)-β-arrestin1 and pcDNA3.1(+)-β-arrestin2[45], pcDNA3.1/Zeo-β-arrestin1-RlucII[46],
342 pcDNA3.1/Zeo-β-arrestin2-RlucII[47], pcDNA3.1(+)-GFP^2-β-arrestin2[48] and pcDNA3.1(+)-rGFP-
343 CAAX[36]. pSpCas9(BB)-2A-GFP (PX458) was a gift from Feng Zhang (Addgene plasmid # 48138;
344 http://n2t.net/addgene:48138; RRID:Addgene_48138) and was described previously[49]. The
345 pcDNA3.1-μ-OR-EYFP plasmid was a gift from the ARPEGE platform (Institut de Génomique
346 Fonctionnelle, Montpellier, France). pcDNA3.1/Hygro(+)-SP-FLAG-μ-OR-RlucII was constructed by
347 PCR amplification of human μ-OR1 tagged with a signal peptide (SP) (MKTIIALSYIFCLVFA) and a
348 variant of the FLAG tag epitope (MDYKDDDDA) from pLVxi2P-SP-FLAG-hμ-OR[27] and then
349 subcloning it into the pcDNA3.1/Hygro(+)GFP10-RlucII vector[50] using Gibson assembly (New
350 England Biolabs) after digestion with NheI + AgeI.
351 The pcDNA3.1(+)-GRK2 and pcDNA3.1(+)-GRK3 constructs were kind gifts from Novo Nordisk A/S
352 (Maaloev, Denmark). All μ-OR, GRK and β-arrestin sequences are the human sequences.
353
354 **Cell lines and culturing**
355 The parental HEK293A and Δβ-arrestin1/2 cell lines were kind gifts from Dr. Asuka Inoue[35]. All cell
356 lines were cultured in DMEM supplemented with 10% FBS and 100 U/ml Penicillin-Streptomycin at
357 37 °C and 5% CO_2 in a humidified incubator.
358

359 **Design and cloning of sgRNAs**

360 sgRNA sequences were identified using the WTSI Genome Editing (WGE) tool by screening exonic
361 regions of the genes *ADRBK1* (RefSeq: NC_000011.10) or *ADRBK2* (RefSeq: NC_000022.11)
362 encoding GRK2 and GRK3, respectively. sgRNAs with low predicted off target effects and binding
363 sites upstream of regions encoding catalytic sites in the GRK proteins were chosen, resulting in the
364 sgRNA sequence 5'-CTTCGACTCATACATCATGA-3' binding in exon 4 within the *ADRBK1* gene and
365 the sgRNA sequence 5'-ATTATTGGACGAGGAGGATT-3' binding in exon 8 within the *ADRBK2* gene.
366 Overhangs for cloning into a BsbI restriction site were placed in the ends of the sgRNAs. sgRNAs
367 were prepared for cloning by incubating 100 μM of reverse complementary strands with T4 PNK in
368 a thermocycler at 37 °C for 30 minutes followed by a 5-minute incubation at 95 °C and ramping
369 down to 25 °C with 5 °C/min. The double stranded sgRNAs were ligated into BsbI digested
370 pSpCas9(BB)-2A-GFP by incubating with T4 DNA ligase for 1 hour at 22 °C. To remove excess non-
371 ligated DNA, the samples were treated with Plasmid-Safe ATP-Dependent DNase for 30 minutes at
372 37 °C.

373

374 **Generation and validation of CRISPR-Cas9 KO cell lines**

375 HEK293A cells were seeded at a density of 2×10^5 cells/well in a 6-well plate and incubated at 37
376 °C and 5% CO_2 in a humidified incubator. Twenty-four hours later cells were transfected with 500
377 ng/well pSpCas9(BB)-2A-GFP encoding the sgRNAs using FuGene6 as the transfection reagent and
378 the cells were incubated at 37 °C and 5% CO_2 in a humidified incubator. Forty-eight hours later,
379 the cells were harvested by trypsination and sorted based on their GFP expression with
380 fluorescence assisted cell sorting (FACS) using a MoFlo Astrios Cell Sorter (Beckman Coulter, Brea,

381 CA, USA). Cells were seeded in 96-well culture plates to isolate single clones and were incubated at
382 37 °C and 5% CO_2 in a humidified incubator until ~70% confluent.
383
384 **IDAA**
385 Single clones were harvested from 96-well plates by trypsination and DNA was extracted using
386 QuickExtract followed by cell lysis (20 min at 65 °C, 10 min at 98 °C) as described previously[32]. A
387 tri-primer PCR described previously[51] was performed using TEMPase Hot Start DNA Polymerase.
388 To amplify the *ADRBK1* locus, the following primers and concentrations were used: 0.05 µM
389 forward primer (5'-AGCTGACCGGCAGCAAAATTGCCAGGCCCTTGGTGGAATTCTATG-3'), 0.5 µM
390 reverse primer (5'-GGACATGCTCAGTGGCACTCTTC-3') and 0.5 µM FAM forward primer (5'-6-FAM-
391 AGCTGACCGGCAGCAAAATTG-3'). For amplification of the *ADRBK2* locus following primers and
392 concentrations were used: 0.05 µM forward primer (5'-
393 AGCTGACCGGCAGCAAAATTGCCTGGGGCATCTCATCCTTCAGC-3'), 0.5 µM reverse primer (5'-
394 CGCCCGGCCTACAGCTTATTTC-3') and 0.5 µM FAM forward primer (5'-6-FAM-
395 AGCTGACCGGCAGCAAAATTG-3'). A touchdown thermocycling program was used with
396 denaturation at 95 °C for 15 min followed by 15 cycles with an annealing temperature of 72 °C
397 ramping down to 58 °C with 1 °C/cycle. Subsequent 24 cycles with 58 °C as annealing temperature
398 was performed ending with elongation at 72 °C for 20 min. For both annealing cycles,
399 denaturation and elongation was performed at 95 °C and 72 °C for 30 s, respectively. IDAA on the
400 resulting PCR products was executed by COBO Technologies Aps (Copenhagen, Denmark).
401
402 **Genome sequencing**

403 DNA from the genome-edited cell lines was extracted as described above for IDAA. The *ADRBK1* or
404 *ADRBK2* regions targeted by the sgRNA were PCR amplified with the forward primers 5'-
405 CCAGGCCCTTGGTGGAATTCTATG-3' (*ADRBK1*) and 5'-CCTGGGGCATCTCATCCTTCAGC-3' (*ADRBK2*)
406 and the same reverse primers as used for IDAA. PCR products were cloned into the pCR4-TOPO TA
407 vectors using the TOPO TA cloning kit and used to transform TOP10 bacteria. DNA from 5-10 single
408 clones was sequenced for each genome-edited cell line to determine the modifications for all
409 alleles.
410
411 **Western blot**
412 Genome-edited HEK293A cells were incubated in 15-cm culture dishes at 37 °C and 5% CO_2 in a
413 humidified incubator until ~90% confluency and harvested with ice cold Cell Dissociation Solution.
414 Cells were centrifuged in a tabletop centrifuge at 4 °C for 5 min at 500 x *g*. Whole cell lysates were
415 prepared from pellets by resuspending in RIPA buffer containing cOmplete protease inhibitor
416 cocktail. Cells were pulse sonicated for 30 s and incubated with end-over-end rotation at 4 °C for
417 60 min. Lysates were centrifuged in a tabletop centrifuge at 4 °C for 10 min at 15,000 x *g*. The
418 supernatant was transferred to a clean microcentrifuge tube and the protein concentrations were
419 determined using Pierce BCA Protein Assay Kit according to the manufacturer's instructions. The
420 absorbance of the samples was measured at 562 nm on an EnSpire Multimode Plate Reader
421 (PerkinElmer), and the values were converted to protein concentrations by interpolation from a
422 bovine serum albumin (BSA) standard curve. Western blot samples were prepared with 50 μg
423 protein in NuPAGE LDS Sample Buffer supplemented with 100 μM dithiothreitol (DTT) and heated
424 for 30 s at 50 °C. Subsequently they were incubated for 15 minutes at room temperature and
425 electrophoresed using 4-20% polyacrylamide gels for 40 min at 200 V. Proteins were transferred

426 onto a polyvinylidene difluoride (PVDF) membrane followed by one hour blocking with 5% skim
427 milk in Tris buffered saline with Tween 20 (TBS-T; 10 mM Tris pH 7.4, 150 mM NaCl, 0.1% Tween
428 20). The PVDF membrane was incubated over night with anti-GRK2 (0.1 μg/ml in TBS-T with 5%
429 skim milk), anti-GRK3 (1:2000 in TBS-T with 5% skim milk), anti-GRK5 (0.5 μg/ml in TBS-T with 5%
430 skim milk), anti-GRK6 (1:1000 in TBS-T with 5% skim milk) or anti-GAPDH (1:5000 in TBS-T with 1%
431 BSA) at 4 °C. The membranes were washed three times with TBS-T and incubated with secondary
432 antibodies for one hour at room temperature with gentle agitation followed by three washes with
433 TBS-T. Blots were developed with HRP substrate and imaged with a FluorChem HD2 system
434 (ProteinSimple, San Jose, CA, USA) or iBright FL1500 (Thermo Fisher Scientific, Waltham, MA,
435 USA).
436
437 **β-arrestin2 recruitment**
438 Parental HEK293A cells or genome-edited cells were transfected with PEI for β-arrestin2
439 recruitment experiments as previously described.[36] 500,000 cells/ml were transfected with the
440 following combinations of plasmids: (1) ebBRET: 20 ng/ml β-arrestin2-RlucII (BRET donor), 500
441 ng/ml rGFP-CAAX (BRET acceptor), pcDNA5/FRT/TO-FLAG-SNAP-μ-OR and pcDNA3.1(+), (2) $BRET^1$:
442 20 ng/ml β-arrestin2-RlucII (BRET donor), 500 ng/ml μ-OR-EYFP (BRET acceptor) and pcDNA3.1(+),
443 and (3) $BRET^2$: μ-OR-RlucII (BRET donor), 20 ng/ml GFP^2-β-arrestin1 or -2 (BRET acceptor) and
444 pcDNA3.1(+). The amounts of pcDNA5/FRT/TO-FLAG-SNAP-μ-OR and μ-OR-RlucII were adjusted
445 for each cell line to equalize the expression: 15 ng/ml for parental HEK293A and ΔGRK2, 10 ng/ml
446 (μ-OR-RlucII) or 20 ng/ml (pcDNA5/FRT/TO-FLAG-SNAP-μ-OR) for ΔGRK2/3 and 30 ng/ml for
447 ΔGRK3. For rescue experiments, 20 ng/ml GRK2 or GRK3 was added in (1). The total DNA amount
448 in all transfections was adjusted to 1 μg/ml with pcDNA3.1(+). 32,000 cells mixed with DNA and

449 PEI were added to each well in poly-D-lysine-coated white, opaque CulturPlate-96 96-well plates
450 (PerkinElmer, Waltham, MA, USA). Forty-eight hours after transfection, cells were washed and
451 incubated in assay buffer (HBSS supplemented with 1 mM $CaCl_2$, 1 mM $MgCl_2$, 20 mM HEPES and
452 0.01% Pluronic F-68, pH 7.4) for 30 min at 37 °C before addition of agonists. For experiments with
453 CMPD101, cells were incubated for an additional 30 min in presence of CMPD101 before agonist
454 addition. Cells were incubated with agonists at 37 °C. For ebBRET/BRET^2 experiments,
455 coelenterazine 400a was added to a final concentration of 2.5 μM and 2 min later BRET was
456 measured on an EnVision 2104 Multilabel Reader (PerkinElmer) using 410/80 nm (donor) and
457 515/30 nm (acceptor) emission filters. BRET^2 ratios were calculated as the ratio of acceptor and
458 donor emission (515 nm/410 nm). For concentration-response curves the buffer response of the
459 parental cells was subtracted. For BRET^1 experiments, coelenterazine h was added to a final
460 concentration of 5 μM for 3 min before measuring BRET on an EnVision 2104 Multilabel Reader
461 using 470/24 nm (donor) and 535/30 nm (acceptor) emission filters. BRET^1 ratios were calculated
462 as the ratio of acceptor and donor emission (535 nm/470 nm). For concentration-response curves
463 the buffer response of the same cell line was subtracted.
464
465 **ELISA**
466 Receptor surface expression in β-arrestin2 recruitment experiments was determined using
467 enzyme-linked immunosorbent assay (ELISA) as previously described[52] with anti-FLAG as primary
468 antibody in a 1:1000 dilution.
469
470 **TR-FRET real-time internalization**

471 Parental HEK293A cells or genome-edited cells were transfected with PEI for real-time
472 internalization experiments with different amounts of pcDNA5/FRT/TO-FLAG-SNAP-μ-OR
473 depending on the cell line (same amounts for each cell line as in β-arrestin2 recruitment
474 experiments) to equalize expression and the total DNA amount was adjusted to 1 μg/ml with
475 pcDNA3.1(+). For rescue experiments, cells were co-transfected with 30 ng/ml GRK2, GRK3, -β-
476 arrestin1, or -β-arrestin2. 14,000 cells mixed with DNA and PEI were added to each well in a poly-
477 D-lysine-coated white, opaque 384-well plates (Greiner Bio-One, Kremsmünster, Austria). Forty-
478 eight hours after transfection, cells were labeled with 10 μl Tag-lite Lumi4-Tb for 60 min at 37 °C in
479 Opti-MEM. After labeling, cells were washed twice with assay buffer (HBSS supplemented with 1
480 mM $CaCl_2$, 1 mM $MgCl_2$, 20 mM HEPES and 0.01% Pluronic F-68, pH 7.4) and incubated for 5 min
481 with 10 μl of 100 μM fluorescein-O'-acetic acid. The donor signal was measured before removing
482 the second wash from the plate and used as a measure of the μ-OR surface expression. For
483 experiments with CMPD101, the compound was added together with fluorescein-O'-acetic acid
484 and the incubation was extended to 30 min. 10 μl agonist was then added and internalization was
485 read immediately after for 90 min in 6 min intervals on an EnVision 2104 Multilabel Reader using a
486 340/60 nm excitation filter and emission was recorded through 520/8 nm (acceptor) and 615/8.5
487 nm (donor) emission filters. Internalization ratios were calculated as the ratio of donor over
488 acceptor emission (615 nm/520 nm) for real-time internalization curves. For concentration-
489 response curves the area under the real-time internalization curves was calculated and the buffer
490 response subtracted. The IC_{50} of CMPD101 inhibition of internalization was determined by fitting
491 the concentration-response curve obtained by subtracting the DAMGO − buffer response in
492 ΔGRK2/3 cells from the DAMGO − buffer response in parental cells.
493

494 **Data analysis and statistics**

495 Data are presented as mean ± SEM of n ≥ 3 independent experiments. Results were analyzed
496 using Prism 7 and 8 (GraphPad Software, San Diego, CA, USA). Differences were determined with
497 regular or repeated measures one-way ANOVA with Dunnett's multiple comparisons test or paired
498 t-test on non-normalized data; $P < 0.05$ was considered significant. In Fig. 1b where data was
499 compared to a reference value without variance (100 ± 0), observations were compared to the
500 reference value using a one sample t-test and the cutoff for what was considered a significant
501 difference was adjusted to $P < 0.05/n$ (n represents the number of compared observations) to
502 account for multiple comparisons.

503

504 **Data Availability**

505 The datasets generated during the current study are available from the corresponding authors on
506 reasonable request.

507

508

509 **References:**

510 1. Hauser, A. S., Attwood, M. M., Rask-Andersen, M., Schiöth, H. B. & Gloriam, D. E. Trends in
511 GPCR drug discovery: new agents, targets and indications. *Nat. Rev. Drug Discov.* **16**, 829–
512 842 (2017).

513 2. Hanyaloglu, A. C. & Zastrow, M. von. Regulation of GPCRs by endocytic membrane
514 trafficking and its potential implications. *Annu. Rev. Pharmacol. Toxicol.* **48**, 537–568 (2008).

515 3. Dahan, A. *et al.* Anesthetic potency and influence of morphine and sevoflurane on
516 respiration in mu-opioid receptor knockout mice. *Anesthesiology* **94**, 824–832 (2001).

517 4. Charbogne, P., Kieffer, B. L. & Befort, K. 15 years of genetic approaches in vivo for addiction
518 research: Opioid receptor and peptide gene knockout in mouse models of drug abuse.
519 *Neuropharmacology* **76**, 204–217 (2014).
520 5. Williams, J. T. *et al.* Regulation of μ-opioid receptors: Desensitization, phosphorylation,
521 internalization, and tolerance. *Pharmacol. Rev.* **65**, 223–254 (2013).
522 6. Wang, Z., Arden, J. & Sadee, W. Basal phosphorylation of μ opioid receptor is agonist
523 modulated and Ca2+-dependent. *FEBS Lett.* **387**, 53–57 (1996).
524 7. Zhang, L. *et al.* Differential μ opiate receptor phosphorylation and desensitization induced
525 by agonists and phorbol esters. *J. Biol. Chem.* **271**, 11449–11454 (1996).
526 8. Yu, Y. *et al.* μ opioid receptor phosphorylation, desensitization, and ligand efficacy. *J. Biol.*
527 *Chem.* **272**, 28869–28874 (1997).
528 9. Deng, H. B. *et al.* Role for the C-terminus in agonist-induced μ opioid receptor
529 phosphorylation and desensitization. *Biochemistry* **39**, 5492–5499 (2000).
530 10. Miess, E. *et al.* Multisite phosphorylation is required for sustained interaction with GRKs
531 and arrestins during rapid μ-opioid receptor desensitization. *Sci. Signal.* **11**, eaas9609
532 (2018).
533 11. Birdsong, W. T., Arttamangkul, S., Bunzow, J. R. & Williams, J. T. Agonist binding and
534 desensitization of the μ-opioid receptor is modulated by phosphorylation of the C-terminal
535 tail domain. *Mol. Pharmacol.* **88**, 816–824 (2015).
536 12. Yousuf, A. *et al.* Role of phosphorylation sites in desensitization of μ-opioid receptor. *Mol.*
537 *Pharmacol.* **88**, 825–835 (2015).
538 13. Raehal, K. M., Schmid, C. L., Groer, C. E. & Bohn, L. M. Functional selectivity at the μ-opioid
539 receptor: implications for understanding opioid analgesia and tolerance. *Pharmacol. Rev.*

540 **63**, 1001–1019 (2011).

541 14. Terman, G. W. *et al.* G-protein receptor kinase 3 (GRK3) influences opioid analgesic
542 tolerance but not opioid withdrawal. *Br. J. Pharmacol.* **141**, 55–64 (2004).

543 15. Glück, L. *et al.* Loss of morphine reward and dependence in mice lacking G protein-coupled
544 receptor kinase 5. *Biol. Psychiatry* **76**, 767–774 (2014).

545 16. Raehal, K. M. *et al.* Morphine-induced physiological and behavioral responses in mice
546 lacking G protein-coupled receptor kinase 6. *Drug Alcohol Depend.* **104**, 187–196 (2009).

547 17. Jaber, M. *et al.* Essential role of beta-adrenergic receptor kinase 1 in cardiac development
548 and function. *Proc. Natl. Acad. Sci.* **93**, 12974–12949 (1996).

549 18. Li, A. H. & Wang, H.-L. G protein-coupled receptor kinase 2 mediates μ-opioid receptor
550 desensitization in GABAergic neurons of the nucleus raphe magnus. *J. Neurochem.* **77**, 435–
551 444 (2001).

552 19. Bailey, C. *et al.* Involvement of PKCα and G-protein-coupled receptor kinase 2 in agonist-
553 selective desensitization of μ-opioid receptors in mature brain neurons. *Br. J. Pharmacol.*
554 **158**, 157–164 (2009).

555 20. Zhang, J. *et al.* Role for G protein-coupled receptor kinase in agonist-specific regulation of
556 mu-opioid receptor responsiveness. *Proc. Natl. Acad. Sci.* **95**, 7157–7162 (1998).

557 21. McPherson, J. *et al.* μ-opioid receptors: correlation of agonist efficacy for signalling with
558 ability to activate internalization. *Mol. Pharmacol.* **78**, 756–766 (2010).

559 22. Schulz, S. *et al.* Morphine induces terminal μ-opioid receptor desensitization by sustained
560 phosphorylation of serine-375. *EMBO J.* **23**, 3282–3289 (2004).

561 23. Just, S. *et al.* Differentiation of opioid drug effects by hierarchical multi-site
562 phosphorylation. *Mol. Pharmacol.* **83**, 633–639 (2013).

563 24. Lau, E. K. *et al.* Quantitative encoding of the effect of a partial agonist on individual opioid
564 receptors by multisite phosphorylation and threshold detection. *Sci. Signal.* **4**, ra52–ra52
565 (2011).
566 25. Pedersen, M. F. *et al.* Biased agonism of clinically approved μ-opioid receptor agonists and
567 TRV130 is not controlled by binding and signaling kinetics. *Neuropharmacology* **166**, 107718
568 (2020).
569 26. Doll, C. *et al.* Deciphering μ-opioid receptor phosphorylation and dephosphorylation in
570 HEK293 cells. *Br. J. Pharmacol.* **167**, 1259–1270 (2012).
571 27. Ehrlich, A. T. *et al.* Biased signaling of the mu opioid receptor revealed in native neurons.
572 *iScience* **14**, 47–57 (2019).
573 28. Celver, J., Xu, M., Jin, W., Lowe, J. & Chavkin, C. Distinct domains of the μ-opioid receptor
574 control uncoupling and internalization. *Mol. Pharmacol.* **65**, 528–537 (2004).
575 29. Ikeda, S., Manami, K. & Fujiwara, S. Cardiotonic agent comprising grk inhibitor. (2007).
576 30. Thal, D. M., Yeow, R. Y., Schoenau, C., Huber, J. & Tesmer, J. J. G. Molecular mechanism of
577 selectivity among G protein-coupled receptor kinase 2 inhibitors. *Mol. Pharmacol.* **80**, 294–
578 303 (2011).
579 31. Lowe, J. D. *et al.* Role of G protein-coupled receptor kinases 2 and 3 in μ-opioid receptor
580 desensitization and internalization. *Mol. Pharmacol.* **88**, 347–356 (2015).
581 32. Lonowski, L. A. *et al.* Genome editing using FACS enrichment of nuclease-expressing cells
582 and indel detection by amplicon analysis. *Nat. Protoc.* **12**, 581–603 (2017).
583 33. Roed, S. N. *et al.* Real-time trafficking and signaling of the glucagon-like peptide-1 receptor.
584 *Mol. Cell. Endocrinol.* **382**, 938–949 (2014).
585 34. Levoye, A. *et al.* A Broad G Protein-Coupled Receptor Internalization Assay that Combines

586 SNAP-Tag Labeling, Diffusion-Enhanced Resonance Energy Transfer, and a Highly Emissive
587 Terbium Cryptate. *Front. Endocrinol. (Lausanne).* **6**, 167 (2015).
588 35. O'Hayre, M. *et al.* Genetic evidence that β-arrestins are dispensable for the initiation of β2-
589 adrenergic receptor signaling to ERK. *Sci. Signal.* **10**, eaal3395 (2017).
590 36. Namkung, Y. *et al.* Monitoring G protein-coupled receptor and β-arrestin trafficking in live
591 cells using enhanced bystander BRET. *Nat. Commun.* **7**, 1–12 (2016).
592 37. Boutros, M. & Ahringer, J. The art and design of genetic screens: RNA interference. *Nat.*
593 *Rev. Genet.* **9**, 554–566 (2008).
594 38. Jung, S.-R., Kushmerick, C., Seo, J. B., Koh, D.-S. & Hille, B. Muscarinic receptor regulates
595 extracellular signal regulated kinase by two modes of arrestin binding. *Proc. Natl. Acad. Sci.*
596 **114**, E5579–E5588 (2017).
597 39. Eichel, K., Jullié, D. & von Zastrow, M. β-Arrestin drives MAP kinase signalling from clathrin-
598 coated structures after GPCR dissociation. *Nat. Cell Biol.* **18**, 303–310 (2016).
599 40. Eichel, K. *et al.* Catalytic activation of β-arrestin by GPCRs. *Nature* **557**, 381–386 (2018).
600 41. Jala, V. R., Shao, W.-H. & Haribabu, B. Phosphorylation-independent beta-arrestin
601 translocation and internalization of leukotriene B4 receptors. *J. Biol. Chem.* **280**, 4880–4887
602 (2005).
603 42. Latorraca, N. R. *et al.* Molecular mechanism of GPCR-mediated arrestin activation. *Nature*
604 **557**, 452–456 (2018).
605 43. Luttrell, L. M. *et al.* Manifold roles of β-arrestins in GPCR signaling elucidated with siRNA
606 and CRISPR/Cas9. *Sci. Signal.* **11**, eaat7650 (2018).
607 44. Milligan, G. & Inoue, A. Genome editing provides new insights into receptor-controlled
608 signalling pathways. *Trends Pharmacol. Sci.* **39**, 481–493 (2018).

609 45. Gabe, M. B. N. *et al.* Human GIP(3-30)NH 2 inhibits G protein-dependent as well as G
610 protein-independent signaling and is selective for the GIP receptor with high-affinity binding
611 to primate but not rodent GIP receptors. *Biochem. Pharmacol.* **150**, 97–107 (2018).
612 46. Zimmerman, B. *et al.* Differential β-arrestin-dependent conformational signaling and
613 cellular responses revealed by angiotensin analogs. *Sci. Signal.* **5**, (2012).
614 47. Quoyer, J. *et al.* Pepducin targeting the C-X-C chemokine receptor type 4 acts as a biased
615 agonist favoring activation of the inhibitory G protein. *Proc. Natl. Acad. Sci.* **110**, E5088–
616 E5097 (2013).
617 48. Vrecl, M., Jorgensen, R., Pogačnik, A. & Heding, A. Development of a BRET2 screening assay
618 using β-arrestin 2 mutants. *J. Biomol. Screen.* **9**, 322–333 (2004).
619 49. Ran, F. A. *et al.* Genome engineering using the CRISPR-Cas9 system. *Nat. Protoc.* **8**, 2281–
620 2308 (2013).
621 50. Leduc, M. *et al.* Functional selectivity of natural and synthetic prostaglandin EP4 receptor
622 ligands. *J. Pharmacol. Exp. Ther.* **331**, 297–307 (2009).
623 51. Yang, Z. *et al.* Fast and sensitive detection of indels induced by precise gene targeting.
624 *Nucleic Acids Res.* **43**, e59–e59 (2015).
625 52. Nørskov-Lauritsen, L., Jørgensen, S. & Bräuner-Osborne, H. N-glycosylation and disulfide
626 bonding affects GPRC6A receptor expression, function, and dimerization. *FEBS Lett.* **589**,
627 588–597 (2015).
628

629 **Author contributions:**

630 T.C.M., M.F.P., J.M.M., M.B. and H.B.-O. participated in research design. T.C.M., M.F.P., J.R,v.S.
631 and S.D.S. conducted experiments. T.C.M., M.F.P., J.R.v.S. and S.D.S. performed data analysis.

632 T.C.M., M.F.P., S.D.S. and H.B.-O. wrote or contributed to drafting the manuscript. All authors
633 edited and approved the final manuscript.
634
635 **Acknowledgements:**
636 We thank Dr. Asuka Inoue for the HEK293 parental and Δβ-arrestin1/2 cell lines and for fruitful
637 discussions and Jens Peter Stenvang for technical assistance with cell sorting. We also thank Eric
638 Paul Bennett for input related to indel detection by amplicon analysis. H.B.-O. acknowledges
639 financial support from the Independent Research Fund Denmark | Medical Sciences (4183-
640 00131A), the Lundbeck Foundation, the Novo Nordisk Foundation (NNF17OC0027004), the
641 Carlsberg Foundation (CF17-0132) and the Toyota Foundation (9310-F). M.F.P. thank the Oticon
642 Foundation (16-0668) and the Knud Højgaards Foundation (16-02-0142) for financial support.
643 T.C.M. acknowledges funding from the European Union's Horizon2020 research and innovation
644 programme under the Marie Sklodowska-Curie grant agreement No 797497. M.B. acknowledge
645 the financial support from a Canadian Institute for Health Research (CIHR) Foundation grant (FDN-
646 148431). M.B. also holds a Canada Research Chair in Signal Transduction and Molecular
647 Pharmacology.
648
649 **Additional Information**
650 **Supplementary information** accompanies this paper at …
651 **Competing Interests**: The authors declare no competing interests.

Table 1. E_{max} (% of parental HEK293A (WT) cells) and pEC_{50} values for μ-OR internalization obtained from fitting concentration-response curves calculated by taking the area under the curve of 90 min internalization time curves to a four-parameter model of agonism. No fit could be obtained for experiments in cells where β-arrestin1 and -2 had been deleted. E_{max} and pEC_{50} values are the mean of 3-5 independent experiments. E_{max} and pEC_{50} in knockout cells are compared to the parental cells by one-way ANOVA with Dunnett's multiple comparisons test. $^{*}P$ = 0.01-0.05, $^{**}P$ = 0.001-0.01, $^{***}P$ < 0.001.

	WT				ΔGRK2				ΔGRK3				ΔGRK2/3			
	E_{max}	SEM	pEC_{50}	SEM	E_{max}	SEM	pEC_{50}	SEM	E_{max}	SEM	pEC_{50}	SEM	E_{max}	SEM	pEC_{50}	SEM
DAMGO	100	5	6.44	0.03	52^{***}	5	6.27	0.06	77^{*}	6	6.43	0.04	31^{***}	9	6.14^{**}	0.15
Fentanyl	100	5	6.94	0.01	38^{***}	5	6.75^{***}	0.04	78^{*}	5	6.81^{***}	0.02	18^{***}	6	7.03^{*}	0.01
Loperamide	100	8	6.96	0.04	47^{***}	7	6.74	0.10	78	8	6.95	0.07	18^{***}	17	6.91	0.08
Morphine	100	15	5.65	0.12	84	37	4.65	0.89	71	14	5.84	0.05	38	12	6.02	0.13

Table 2. E_{max} (% of parental HEK293A (WT) cells) and pEC_{50} values for β-arrestin2-RlucII recruitment to the plasma membrane measured by ebBRET after 6 min of μ-OR stimulation. The values are obtained from fitting concentration-response curves to a four-parameter model of agonism. E_{max} and pEC_{50} values are the mean of 3-4 independent experiments. E_{max} and pEC_{50} in knockout cells are compared to the parental cells by one-way ANOVA with Dunnett's multiple comparisons test. $^{*}P$ = 0.01-0.05, $^{**}P$ = 0.001-0.01.

	WT				ΔGRK2				ΔGRK3				ΔGRK2/3			
	E_{max}	SEM	pEC_{50}	SEM	E_{max}	SEM	pEC_{50}	SEM	E_{max}	SEM	pEC_{50}	SEM	E_{max}	SEM	pEC_{50}	SEM
DAMGO	100	8	6.56	0.05	59^{*}	9	6.41	0.15	107	10	6.4	0.05	38^{**}	8	6.56	0.09
Fentanyl	100	9	6.99	0.1	57^{*}	7	6.78	0.16	107	10	6.93	0.06	38^{**}	13	7.32	0.12
Loperamide	100	14	6.95	0.11	51	16	6.76	0.28	102	12	6.77	0.02	42^{*}	13	6.65	0.36
Morphine	100	13	5.78	0.35	69	46	n.d.		97	23	n.d.		74	27	n.d.	

Figure 1

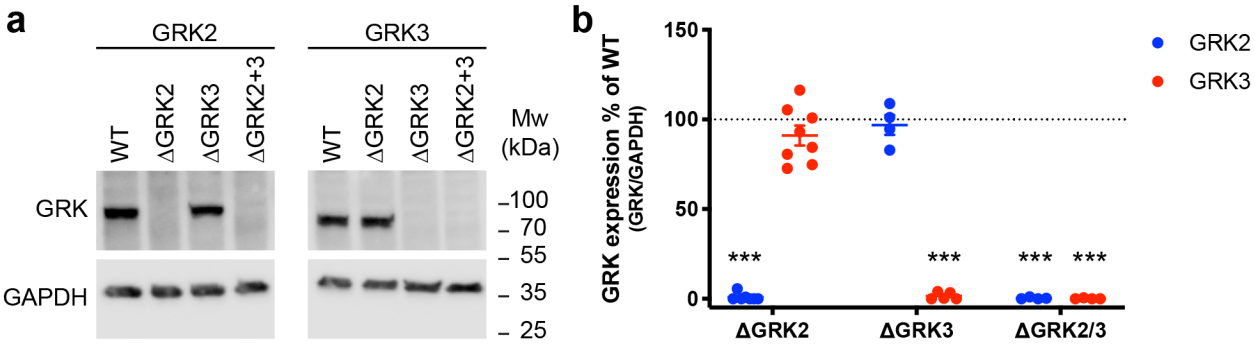

Figure 1. Validation of CRISPR/Cas9 knock-out cell lines. (**a**) Western blot analysis of full-length GRK2 or GRK3 expression in parental or genome-edited cell lines with deletion of GRK2, GRK3 or GRK2/3. The anti-GRK2 and anti-GRK3 antibodies target a site C-terminal to the site that is genetically modified. GAPDH expression is detected to ensure equal loading. Full-length blots are presented in Supplementary Figure 1. (**b**) Quantification of anti-GRK2 and anti-GRK3 western blots after normalization to the GAPDH signal. Mean ± SEM of 4-8 independent experiments. Expression in each of the KO cell lines was compared to the parental cells by one sample t-test using a reference value of 100 and the cutoff for what was considered a significant difference was adjusted to $P < 0.05/n$ (n corresponds to the number of observations) to correct for multiple comparisons. ***$P < 0.001/n$.

Figure 2

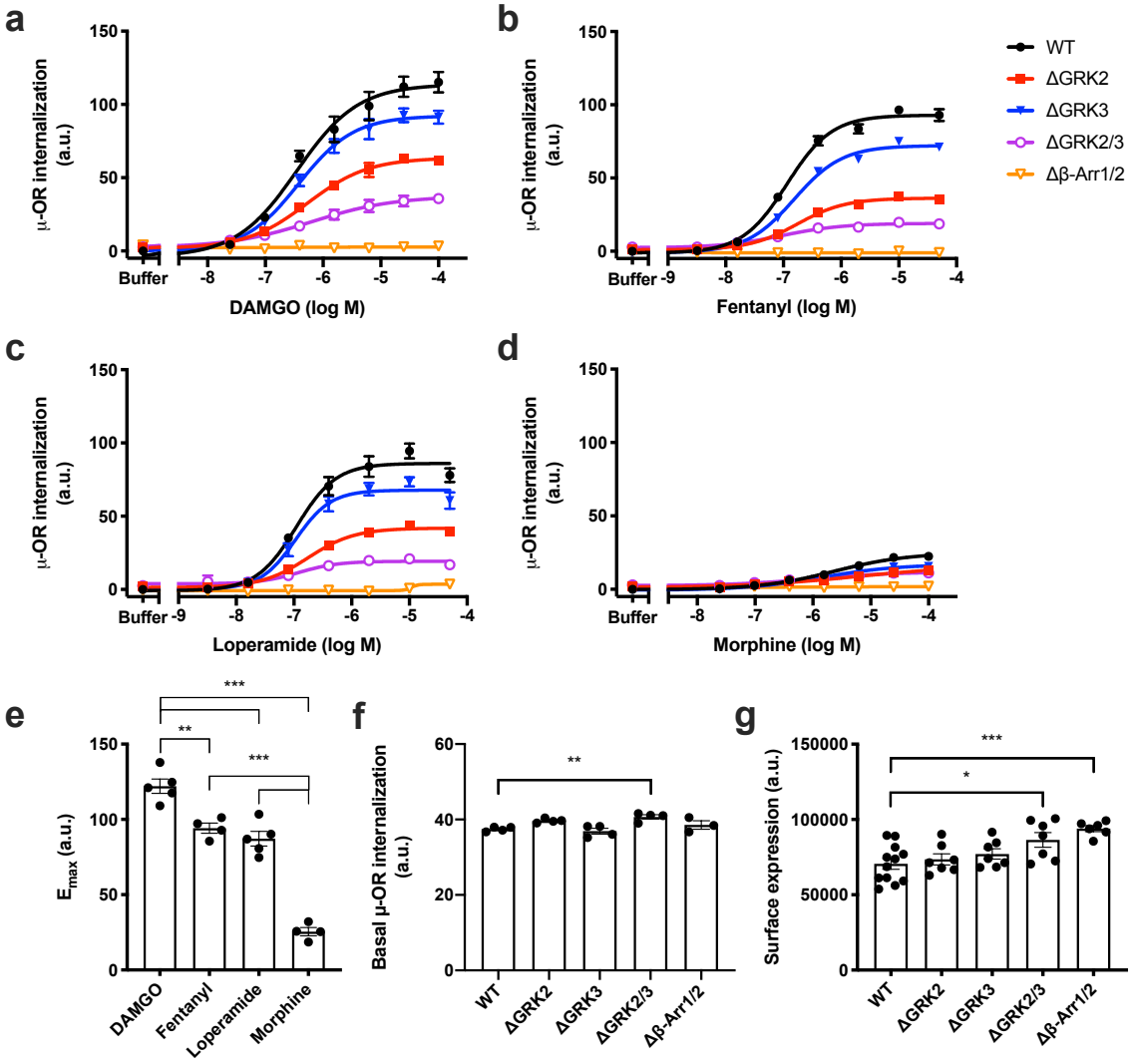

Figure 2. Agonist-induced internalization of μ-OR in genetically modified cell lines. Internalization of μ-OR in response to a range of concentrations of (**a**) DAMGO, (**b**), fentanyl (**c**) loperamide, or (**d**) morphine in parental HEK293A (WT) cells or HEK293A cell lines with deletion of GRK2 (ΔGRK2), GRK3 (ΔGRK3), GRK2 and -3 (ΔGRK2/3) or β-arrestin1 and -2 (Δβ-Arr1/2). Data represent the mean ± SEM of the area under the curve of 90 min real-time internalization experiments after subtraction of the buffer response in parental cells from 3-5 independent experiments carried out in duplicate. Error bars not shown lie within the dimension of the symbol. (**e**) E_{max} of agonist responses in parental cells. Statistical comparison by one-way ANOVA with Dunnett's multiple

comparisons test. (**f**) Basal μ-OR internalization determined by taking the area under the curve of the buffer responses. (**g**) μ-OR cell surface expression determined by measuring donor signals in absence of acceptor. (**e-g**) Data represent the mean of individual experiments (circles) as well as the mean ± SEM (columns) from 4-5 (**e**), 3-4 (**f**) or 6-9 (**g**) independent experiments with 2 (**e**), 4-8 (**f**) or 32 (**g**) replicates per experiment. (**f-g**) Values in knockout cells were compared to the parental cells by one-way ANOVA with Dunnett's multiple comparisons test. *P = 0.01-0.05, **P = 0.001-0.01, ***P < 0.001. a.u., arbitrary units.

Figure 3

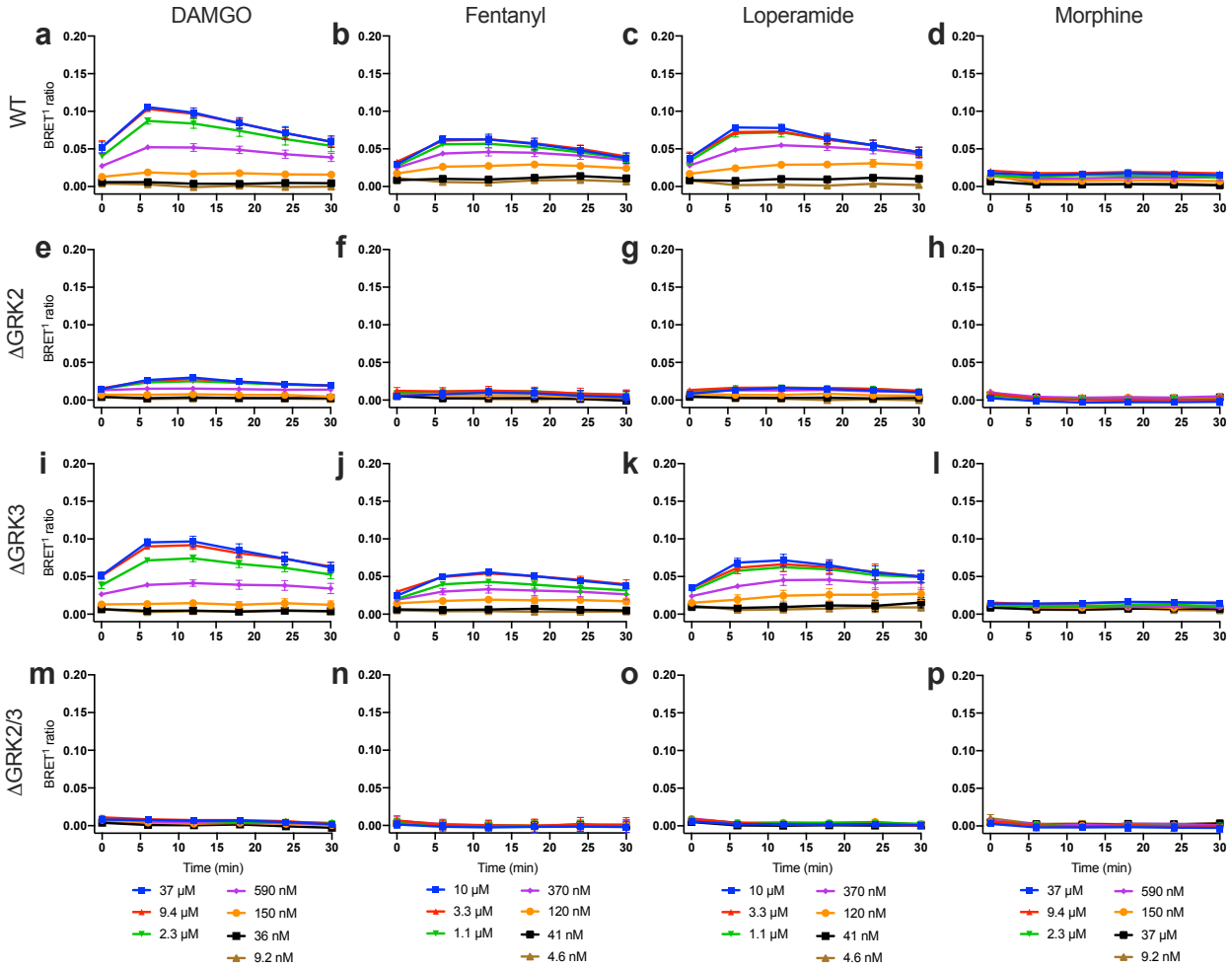

Figure 3. Time course of β-arrestin2 recruitment to μ-OR in GRK knockout cell lines. Recruitment of β-arrestin2-RlucII to μ-OR-EYFP in response to stimulation of μ-OR by a range of concentrations of DAMGO, fentanyl, loperamide or morphine in parental (WT) cells (**a-d**), ΔGRK2 cells (**e-h**), ΔGRK3 cells (**i-l**) or ΔGRK2/3 cells (**m-p**). Data represent mean ± SEM of the $BRET^1$ ratio after buffer subtraction from 3 independent experiments carried out in duplicate. Error bars not shown lie within the dimension of the symbol.

Figure 4

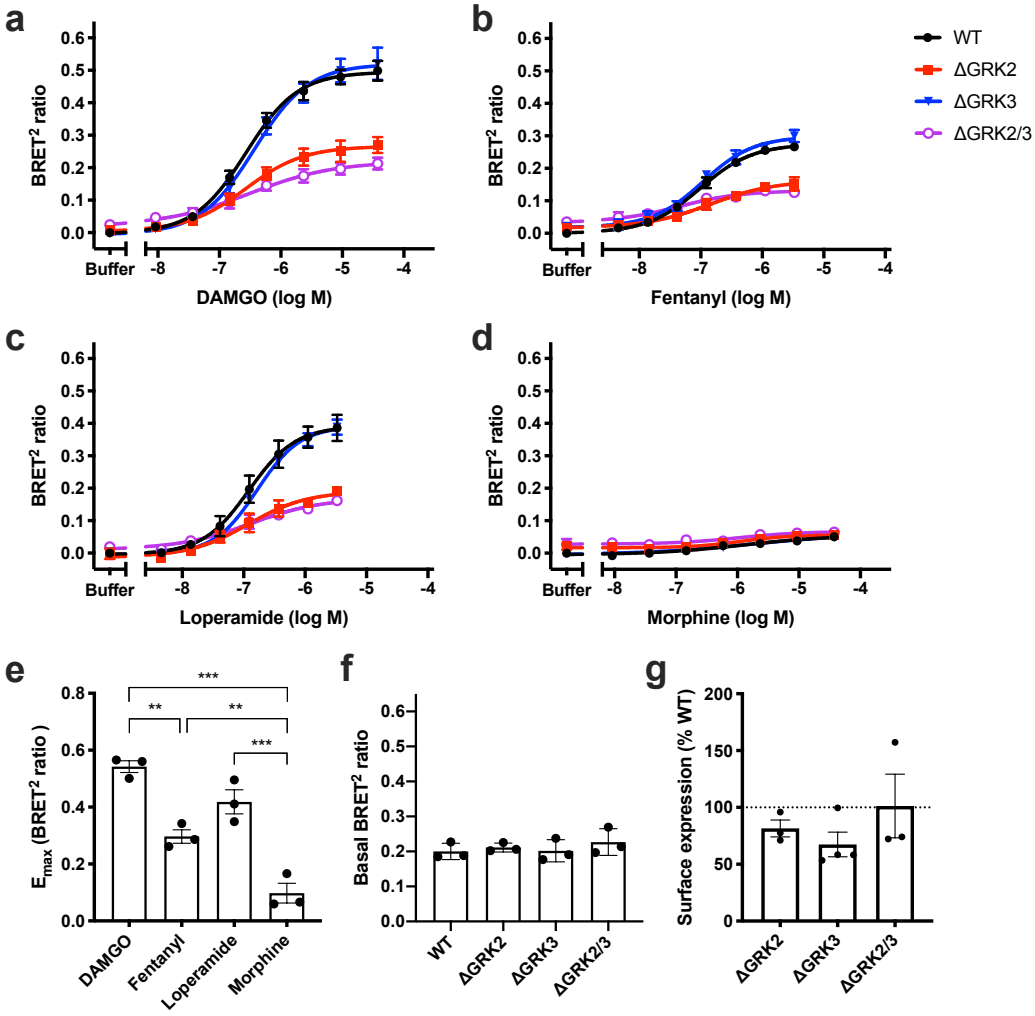

Figure 4. β-arrestin2 recruitment of μ-OR in genetically modified cell lines. Recruitment of β-arrestin2-RlucII to the cell membrane monitored by ebBRET in response to 6 min stimulation of μ-OR by a range of concentrations of (**a**) DAMGO, (**b**) fentanyl, (**c**) loperamide, or (**d**) morphine in parental HEK293A (WT) cells or HEK293A cell lines with deletion of GRK2 (ΔGRK2), GRK3 (ΔGRK3), or GRK2 and -3 (ΔGRK2/3). Data represent the mean ± SEM of the $BRET^2$ ratio after subtraction of the buffer response in parental cells from 3-4 independent experiments carried out in duplicate. Error bars not shown lie within the dimension of the symbol. (**e**) E_{max} of agonist responses in parental cells. Statistical comparison by one-way ANOVA with Dunnett's multiple comparisons test. $^{**}P$ = 0.001-0.01, $^{***}P < 0.001$. (**f**) Basal β-arrestin2 recruitment determined as the buffer

response. (**g**) μ-OR surface expression measured by ELISA and normalized to expression in parental cells. (**e-g**) Data represent the mean of individual experiments (circles) and the mean ± SEM (columns) from 3 (**e-f**) or 3-4 (**g**) independent experiments with 2 (**e**), 6-8 (**f**) or 3 (**g**) replicates per experiment. (**f-g**) Values in knockout cells were compared to the parental cells by one-way ANOVA with Dunnett's multiple comparisons test and no significant differences were found ($P > 0.05$).

Figure 5

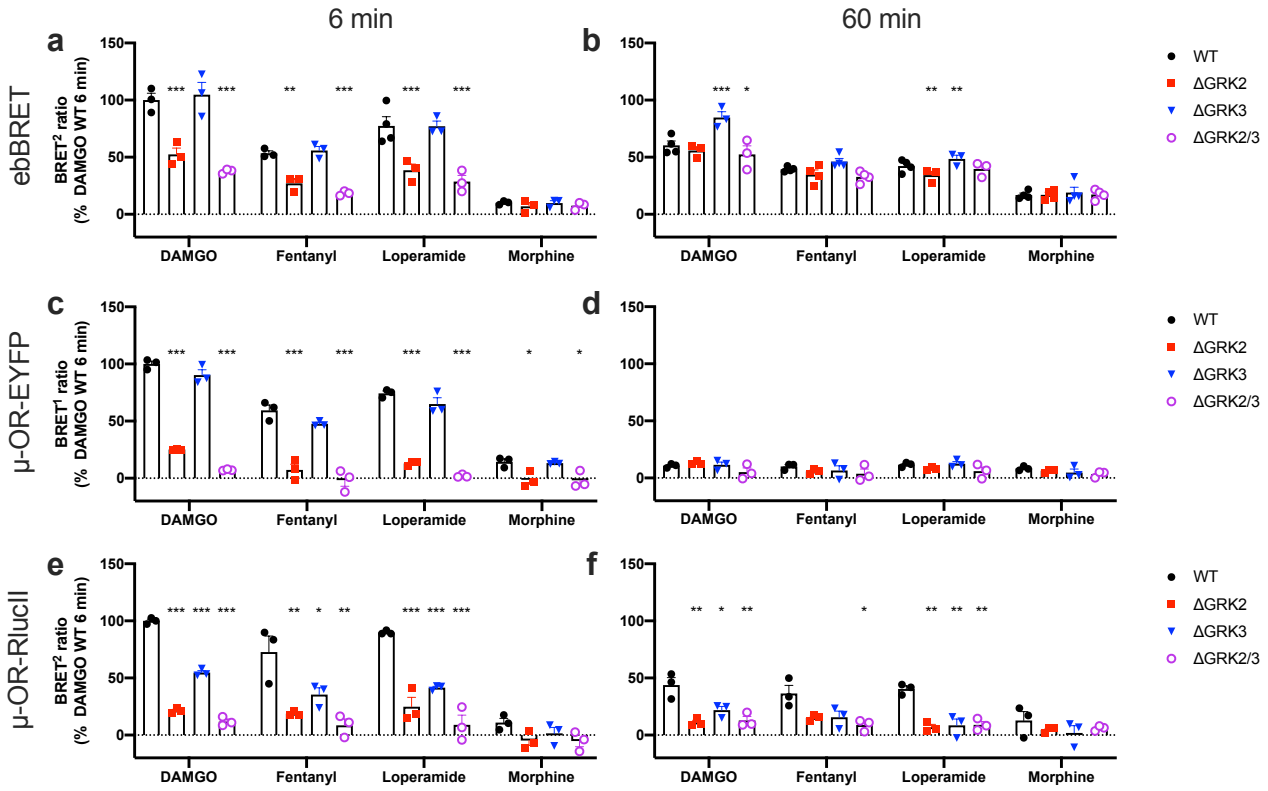

Figure 5. Time dependence of β-arrestin2 recruitment of μ-OR in ΔGRK cell lines. Recruitment of β-arrestin2 after 6 min (**a**, **c**, **e**) or 60 min (**b**, **d**, **f**) stimulation by saturating concentrations of DAMGO (37.5 μM), fentanyl [3.3 μM (**a-b**) or 10 μM (**c-f**)], loperamide [3.3 μM (**a-b**) or 10 μM (**c-f**)] or morphine (37.5 μM) measured by three different assays: ebBRET (**a-b**), recruitment of β-arrestin2-RlucII to μ-OR-EYFP (**c-d**), or recruitment of GFP^2-β-arrestin2 to μ-OR-RlucII. Data represent the mean of individual experiments (circles) as well as the mean ± SEM (columns) after buffer subtraction and normalization to the maximum response in parental (WT) cells stimulated with DAMGO for 6 min from 3-4 independent experiments performed in duplicate. BRET ratios in knockout cells were compared with parental cells by repeated measures one-way ANOVA with Dunnett's multiple comparisons test, except for ebBRET assay with 60 min loperamide stimulation,

which was compared by mixed-effects analysis with Dunnett's multiple comparisons test. *P = 0.01-0.05, **P = 0.001-0.01, ***P < 0.001.

Figure 6

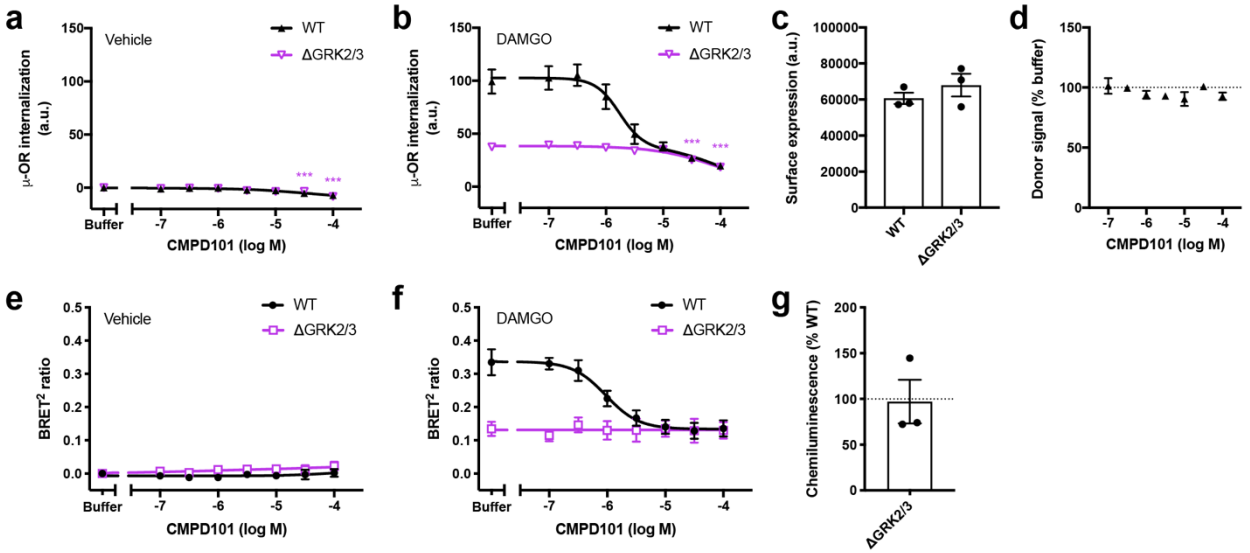

Figure 6. GRK2/3 inhibition and off-target effects by CMPD101. Effect of a range of CMPD101 concentrations on (**a**) basal (vehicle treated) or (**b**) 100 μM DAMGO induced μ-OR internalization and (**e**) basal (vehicle treated) or (**f**) 37.5 μM DAMGO stimulated β-arrestin2 recruitment in parental HEK293A (WT) cells or HEK293A cell lines with deletion of GRK2 and -3 (ΔGRK2/3). β-arrestin2 recruitment was measured by ebBRET after 6 min stimulation of μ-OR. Data represent the mean ± SEM after buffer (vehicle treated) or vehicle (DAMGO treated) subtraction from 3 independent experiments carried out in duplicate. μ-OR surface expression was determined from donor signals in absence of acceptor for internalization experiments (**c**) and by ELISA for β-arrestin2 recruitment experiments (**g**). Data points represent the mean of individual experiments and bars represent the mean ± SEM from three independent experiments with 32 (internalization) or 3 (ELISA) replicates per experiment. In (**g**) data were normalized to expression in parental cells. (**d**) Effect of a range of CMPD101 concentrations on donor signals in absence of acceptor. An unaffected donor signal indicates that the compound does not interfere with the assay. Data represent the mean ± SEM from 3 independent experiments carried out in duplicate. Effect of different CMPD101 concentrations on ΔGRK2/3 cells in (**a**), (**b**), (**d**), (**e**) and (**f**) was compared to

buffer by one-way repeated measures ANOVA with Dunnett's multiple comparisons test before normalization. Expression in parental and ΔGRK2/3 cells in (**c**) and (**g**) was compared by ratio paired t-test before normalization. ***$P < 0.001$. a.u., arbitrary units.